

Nuclear magnetic resonance in a modulated effective field

A. E. Mefed

Institute of Radio Engineering and Electronics, Academy of Sciences of the USSR, Moscow

(Submitted 1 June 1983)

Zh. Eksp. Teor. Fiz. 86, 302–311 (January 1984)

The paper reports the discovery and investigation of the phenomenon of nuclear magnetic resonance (NMR) in the effective magnetic field H_{eff} acting in a doubly rotating coordinate system (DRCS). The H_{eff} was produced by modulating the effective field H_{eff} in the rotating coordinate system. The resonance was observed on the ^1H nuclei in H_2O and the ^{19}F nuclei in CaF_2 , and was recorded by measuring the longitudinal component of the nuclear magnetization with respect to the constant field H_0 . The dependence of the NMR line width in the DRCS on the angle θ' between H'_{eff} and H_{eff} was investigated in CaF_2 for the "magic" orientation of the H_{eff} field. It was found that further suppression of the dipole line width occurs under these conditions, and that this suppression is most effective when $\theta' = \arccos(\frac{3}{5})^{1/2} \approx 39^\circ$ and $\theta' \approx 90^\circ$. In the first case it was possible to narrow the line down to 70 Hz under conditions when the chemical NMR frequency shift was reduced by a factor of $\sqrt{5}$; in the second case, down to 10 Hz upon the suppression of the chemical shift and the inhomogeneous broadening. The results are in good agreement with theory. Nuclear magnetization trapping by the H'_{eff} field ("spin-locking" in the DRCS) has been realized, and a method of measuring the nuclear spin-lattice relaxation time in this field has been developed which furnishes a continuous relaxation curve during one sweep. The possibility of using this method to study slow atomic-molecular motions is discussed.

INTRODUCTION

Experiments in which strong coherent pulsed radio-frequency (RF) fields are used have found wide application in modern NMR spectroscopy.¹⁻⁴ They have, in particular, led to sharp sensitivity and resolving-power increases in the recording of NMR spectra in solids, and have also made the recording of slow atomic-molecular motions possible. In these experiments the NMR signal is recorded at a frequency equal to the RF field frequency, which, in practice, is possible only in the intervals between the RF pulses. But the presence of such intervals ("windows") does not, in a number of cases, allow us to realize the optimal experimental conditions. For example, the cycle duration increases significantly, which worsens the resolution⁴; there appear RF field harmonics, which speed up the magnetization damping⁵⁻⁷; and the RF power level required becomes much higher.⁸⁻¹⁰

A fundamentally different method of detecting NMR was recently developed¹¹ in which what is recorded is the nuclear magnetization component longitudinal with respect to the constant field H_0 (and not the transverse component, as is usually done). In this method the signal is picked up during the time of action of the strong continuous RF field, the reception being realized directly at the NMR frequency in the effective field H_{eff} acting in the rotating coordinate system (RCS). This frequency is significantly lower than the RF field frequency, which makes the simultaneous operation of the transmitter and the receiver possible. As shown in Ref. 11, this method furnishes the NMR spectra of solid samples with increased resolution, and right away in the final form, with no need for a Fourier transformation. But the minimum NMR line width attained in this way (about 300 Hz in CaF_2 (Ref. 11)) is significantly greater than

the width attained in the pulsed methods.⁴ In Ref. 12 a method, based on strong resonance saturation in the RCS, is proposed for the further suppression of the residual NMR line broadening in such experiments. By its physical meaning this idea is connected with the phenomenon of nuclear magnetic resonance in a doubly rotating coordinate system (DRCS). The present investigation was devoted to the detection of this phenomenon and the use of it for the purpose of further narrowing down the NMR line in solids, as well as to the measurement of the nuclear spin-lattice relaxation in the effective field acting in the DRCS. Preliminary results of the investigation were published in Ref. 13.

1. PRINCIPLE AND METHOD OF NMR DETECTION IN THE DRCS

Let a solid sample containing nuclear spins I be acted upon by a strong polarizing field H_0 and a strong RF field $2H_1 \cos \omega t$ oriented respectively along the Z and X axes in the laboratory coordinate system (LCS), and such that $\omega \approx \omega_0 \equiv \gamma H_0$ and $H_0 \gg H_1 \gg H_L$, where γ is the nuclear gyromagnetic ratio and H_L is the local field in the LCS. Then in the oblique RCS (rotation with frequency ω about the Z axis) the spins I are acted upon by an effective static magnetic field $H_{\text{eff}} \parallel z$ having an intensity $H_{\text{eff}} = (\Delta^2 + H_1^2)^{1/2}$, and making with the Z axis an angle of $\theta = \arccos(\Delta / H_{\text{eff}})$, where $\Delta = H_0 - \omega / \gamma$ (Fig. 1).^{1,14} To observe the NMR directly in the RCS in the quasistationary regime,¹¹ we apply in the direction perpendicular to the z axis a second RF field $H_x(t) = 2H_{2\perp} \cos(\Omega t + \varphi)$ with frequency $\Omega \approx \Omega_0 \equiv \gamma H_{\text{eff}}$, which has a typical value of ~ 100 – 300 kHz. To produce this field, it is convenient to use the shallow angle modulation that arises with this frequency of the effective field H_{eff} upon

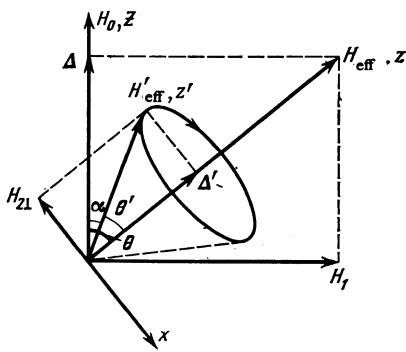


FIG. 1. Geometry of the effective magnetic fields in the rotating and doubly rotating coordinate systems.

the modulation of the frequency ω or amplitude H_1 of the RF field.¹¹ The field $H_x(t)$ is used to excite the component $M_{\rho\perp}$ of the sample magnetization \mathbf{M} , i.e., the component perpendicular to, and rotating with frequency Ω about, the field \mathbf{H}_{eff} . The relation between $M_{\rho\perp}$ and the experimentally measurable magnetization component $M_z(t)$ is given by the formula

$$M_z(t) = M_{\rho\parallel} \cos \theta + \sin \theta [u_\rho \cos(\Omega t + \varphi) + v_\rho \sin(\Omega t + \varphi)], \quad (1)$$

where $M_{\rho\parallel}$ is the \mathbf{M} component parallel to the field \mathbf{H}_{eff} , and u_ρ and v_ρ are mutually orthogonal components of $M_{\rho\perp}$, u_ρ coinciding in direction with the effective circularly polarized component $H_{2\perp}$ of the $H_x(t)$ field (Fig. 1). The components u_ρ and v_ρ induce in the pickup coil, which is oriented along the Z axis and tuned to the frequency Ω , NMR dispersion and absorption signals in the RCS.¹¹

By analogy with the strong RF field $2H_1 \cos \omega t$ widely used in modern NMR spectroscopy, it is natural to consider the phenomenon of nuclear magnetic resonance in the RCS in the case of a strong $H_x(t)$ field satisfying the condition

$$H_{L\rho} \ll H_{2\perp} \ll H_{\text{eff}}, \quad (2)$$

where $H_{L\rho}$ is the local field in the RCS. To do this, let us go over to an oblique DRCS (the second rotation occurring with frequency Ω about the z axis).^{11, 15} In the DRCS the spins I are acted upon by a new static effective magnetic field $\mathbf{H}'_{\text{eff}} \parallel z'$ having an intensity $H'_{\text{eff}} = [(\Delta')^2 + H_{2\perp}^2]^{1/2}$, and making with the z axis an angle $\theta' = \arccos(\Delta'/H'_{\text{eff}})$, where $\Delta' = H_{\text{eff}} - \Omega/\gamma$ (Fig. 1). It is clear that the NMR phenomenon can, in principle, occur at the frequency $\Omega'_0 = \gamma H'_{\text{eff}}$ in the DRCS, just as it occurs in the LCS at the frequency ω_0 and in the RCS at the frequency Ω_0 , where $\Omega'_0 \ll \Omega_0 \ll \omega_0$. In the DRCS the dipole broadening of the resonance line is naturally determined by the secular—with respect to the z' axis—part of the nuclear dipole-dipole interaction $\hat{\mathcal{H}}_{\text{dpp}}^{(0)}$.

Let us assume that the condition for the “magic” angle $\theta = \theta_m = \arccos(1/\sqrt{3})$ is fulfilled in the RCS. In this case the secular—with respect to the z axis—part of the nuclear dipole-dipole interaction ($\hat{\mathcal{H}}_{\text{dp}}^{(1)}$), as separated out in first-order perturbation theory, vanishes. This leads in the RCS to a sharp narrowing of the NMR line, the residual width of which is determined only by the second order correction $\hat{\mathcal{H}}_{\text{dp}}^{(2)}$ (Refs. 11 and 16). In this case the Hamiltonian $\hat{\mathcal{H}}_{\text{dpp}}^{(0)}$, in the DRCS also amounts to a small correction $\hat{\mathcal{H}}_{\text{dpp}}^{(2)}$,

which can be obtained from $\hat{\mathcal{H}}_{\text{dp}}^{(2)}$ by performing the appropriate transformation of the coordinate system.¹² It is shown in Ref. 12 that the NMR line in the DRCS should undergo further narrowing at certain values of the angle θ' .

Thus, the distinguishing feature of nuclear magnetic resonance in the DRCS is the further lowering of the resonance frequency (practically to $\Omega'_0 \sim 1-10$ kHz) and the possibility of further suppression of the resonance-line broadening in solids.

Let us now proceed to describe the quasistationary method used in our investigation to observe NMR in the DRCS. Let us assume that the field $2H_{2\perp} \cos(\Omega t + \varphi)$ is produced through the modulation of the frequency ω , and that the magnetization \mathbf{M} is oriented along \mathbf{H}_{eff} (how the latter can be achieved in practice will be stated a little later). Further, let the signal with frequency Ω , with the aid of which the RF field is frequency-modulated be, in its turn, frequency or amplitude modulated with frequency $\Omega' \approx \gamma H'_{\text{eff}}$. It is clear that the field $2H_{2\perp} \cos(\Omega t + \varphi)$ then becomes frequency- or amplitude-modulated, with a modulation depth of $\delta\Omega$ or $\delta H_{2\perp}$. This leads to the modulation of the effective field \mathbf{H}'_{eff} in the DRCS in magnitude and direction. The angle modulation of the \mathbf{H}'_{eff} field is equivalent to the appearance in the DRCS of a variable magnetic field $\mathbf{H}'_x(t) = 2H_{3\perp} \cos(\Omega' t + \varphi')$ oriented perpendicularly to the z' axis (Fig. 2). Here $2H_{3\perp} = (\delta\Omega/\gamma)\sin\theta'$ in the case of frequency modulation and $2H_{3\perp} = \delta H_{2\perp} \cos\theta'$ in the case of amplitude modulation.

When the resonance condition

$$\Omega' = \Omega'_0 = \gamma H'_{\text{eff}} \quad (3)$$

is fulfilled in the DRCS, the field $\mathbf{H}'_x(t)$ deflects the vector \mathbf{M} from the z' axis, as a result of which the magnetization acquires a nonzero component $M_{\rho\perp}$ perpendicular to, and rotating with frequency Ω' about, the \mathbf{H} field (Fig. 2). Let us resolve this component into two components, one of which ($u_{\rho\rho}$) is in phase with the effective circularly polarized component $H_{3\perp}$ of the $\mathbf{H}'_x(t)$ field, while the other ($v_{\rho\rho}$) lags in phase by $\pi/2$. The components $u_{\rho\rho}$ and $v_{\rho\rho}$ have been introduced by analogy with the conventional description of NMR,¹⁷ and characterize respectively the NMR dispersion and absorption signals in the DRCS. In the case of modulation of, for example, the frequency Ω of the $H_{2\perp}$ field we have

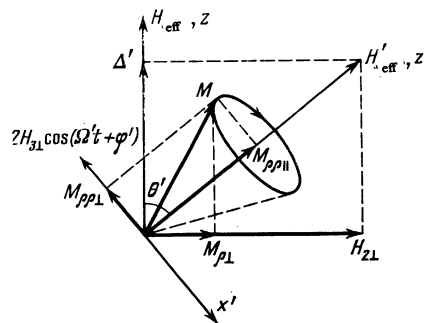


FIG. 2. Principle underlying the excitation of NMR in the doubly rotating coordinate system in the quasistationary regime.

$$M_x = -v_{pp} \sin(\Omega't + \varphi') - u_{pp} \cos(\Omega't + \varphi'),$$

$$M_y = -v_{pp} \cos(\Omega't + \varphi') + u_{pp} \sin(\Omega't + \varphi'), \quad M_z = M_{pp\parallel}.$$

Performing successive coordinate transformations from the DRCS into the LCS, we obtain for the sought quantity $M_z(t)$ the expression

$$M_z(t) = M_{pp\parallel} \cos \theta' \cos \theta + \cos \theta \sin \theta' [u_{pp} \cos(\Omega't + \varphi') + v_{pp} \sin(\Omega't + \varphi')] + M_{pp\parallel} \sin \theta \sin \theta' \cos(\Omega t + \varphi) + 1/2 \sin \theta (1 - \cos \theta') \{u_{pp} \cos[(\Omega - \Omega')t + \varphi - \varphi'] - v_{pp} \sin[(\Omega - \Omega')t + \varphi - \varphi']\} - 1/2 \sin \theta (1 + \cos \theta') \{u_{pp} \cos[(\Omega + \Omega')t + \varphi + \varphi'] + v_{pp} \sin[(\Omega + \Omega')t + \varphi + \varphi']\}. \quad (4)$$

Here the term with the frequency Ω characterizes the NMR in the RCS in the field H_{eff} [cf. (1)], while the side resonances occurring at the frequencies $\Omega \pm \Omega'$ characterize the NMR in the DRCS in the field H'_{eff} . The appearance of the latter resonances can be qualitatively explained by the fact that, during the precession of the magnetization \mathbf{M} about the z' axis, the component $M_{\rho\perp}$ and, hence, $M_z(t)$ undergoes modulation with frequency Ω' (Fig. 2). As can be seen from (4), the side resonances contain a simple combination of NMR absorption and dispersion signals, v_{pp} and u_{pp} respectively, in the DRCS. Each of these signals can clearly be isolated in its pure form, and this was experimentally realized by us.

It can also be seen from (4) that the spectrum of $M_z(t)$ contains a component directly at the NMR frequency Ω' in the DRCS. But this frequency is significantly lower than $\Omega \pm \Omega'$; therefore, the recording of $M_z(t)$ at the frequency Ω' is less convenient.

Similarly, we can find the components $M_x(t)$ and $M_y(t)$ used in the standard procedure for recording NMR in the LCS at the frequency ω . As calculations show, these components contain, besides the band with frequency ω , side bands at the frequencies $\omega \pm \Omega$, $(\omega \pm \Omega) \pm \Omega'$, and $\omega \pm \Omega'$, which can, in principle, also be used to observe the NMR in the RCS and DRCS. But it is very difficult to record them because of the presence of the high-power signal with the close frequency ω .

It should be noted that there are in the RCS and DRCS, besides the components $H_{2\perp}$ and $H_{3\perp}$ of the fields with frequencies Ω and Ω' , components $H_{2\parallel}$ and $H_{3\parallel}$ parallel to the z and z' axes respectively. They can induce parametric resonances,¹⁸ but under the conditions of our experiments ($H_{2\perp}, H_{2\parallel} \ll H_{\text{eff}}; H_{3\perp}, H_{3\parallel} \ll H'_{\text{eff}}$) their influence can be neglected. We can, if necessary, eliminate the components $H_{2\parallel}$ and $H_{3\parallel}$ through the simultaneous frequency and amplitude modulations, with a definite phase shift between them, of the corresponding RF field.

In order to obtain the strongest NMR signals in the DRCS, we must orient along the H'_{eff} field as great a part as possible of the equilibrium sample magnetization \mathbf{M}_0 stored in the \mathbf{H}_0 field. This can be achieved by switching on the modulated H_1 field either adiabatically or suddenly. In the first variant, which is suitable when $|\Delta| \gg H_L$, the H'_{eff} field is also switched on adiabatically (because of the smooth growth of the angles θ and θ' from their zero values to the

final values). This yields the result $M_{\rho\parallel} \approx M_0$, with the magnetization oriented against the H'_{eff} field when $\Delta > 0$ and along this field when $\Delta < 0$. In the second variant, which is suitable for all Δ and $\Delta' \lesssim \gamma H_{2\perp}$, the field $H_{2\perp}$ is switched on suddenly, which ensures that $M_{\rho\parallel} = M_0 \cos \alpha$, where α is the angle between the directions of the H'_{eff} and \mathbf{H}_0 fields at the moment the transmitter is started, which angle is determined by the initial phase φ of the field $2H_{2\perp} \cos(\Omega t + \varphi)$ (Fig. 1). For the optimum value of φ we have $\alpha_{\text{min}} = \theta - \theta'$ (Fig. 1); therefore, when $\theta = \theta'$ the situation can be realized in which the initial direction of the H'_{eff} field coincides with the axis $Z \parallel \mathbf{H}_0, \mathbf{M}_0$. It is clear that in this case the magnetization M_0 will be "trapped" by the H'_{eff} field (i.e., $\mathbf{M}_0 \parallel z'$ and $M_{\rho\parallel} = M_0$), and will rotate together with this field about the z axis with frequency Ω . In both variants the procedure for orienting the magnetization \mathbf{M}_0 along the H'_{eff} field, i.e., for "spin locking" in the DRCS is similar to the well known method, widely used to measure the nuclear spin-lattice relaxation time $T_{1\rho}$ in the RCS,^{1,2} of spin locking in the field \mathbf{H}_1 .

To traverse in the DRCS the resonance region determined by the condition (3) and obtain the NMR absorption or dispersion spectrum in the DRCS, it is convenient to smoothly vary the frequency Ω or Ω' . Of these two possibilities, the Ω' -sweep method is more convenient, since it guarantees a linear sweep of the spectrum, and enables us to fix both of the angles θ and θ' . The latter is important for the realization of the optimal conditions for the suppression of the dipole-dipole interactions in solids.

2. EXPERIMENTAL RESULTS AND THEIR DISCUSSION

A. Experimental conditions

The experiments were performed on a quasistationary spectrometer that allows the direct detection of NMR in the RCS, and records the longitudinal—with respect to the \mathbf{H}_0 field—component of the nuclear magnetization, which we modified in the manner described in Sec. 1. The transmitter of the spectrometer operated at a frequency of 14 MHz; the receiver, at a frequency of ≈ 100 kHz. The resonance was observed on the ^1H nuclei in water and the ^{19}F nuclei in a CaF_2 single crystal (orientation: $[111] \parallel \mathbf{H}_0$) with $H_0 \approx 0.35$ T and at temperatures of 293 and 78 K. The sample volumes were about 30 mm.³ All the experiments were performed under conditions when $\theta = \theta_m$ and $\Omega_0/2\pi = 100$ kHz, i.e., the \mathbf{H}_1 -field intensities in the cases of the ^{19}F and ^1H nuclei were 2.04 and 1.92 mT respectively. The instability of the H_1 field over the experimental period (about 8 sec) did not exceed 0.2%, and the inhomogeneity of this field in the sample volume was about 0.1%. The spectrometer receiver contained two parallel channels—a relatively broad-band channel that transmitted the frequencies Ω and $\Omega \pm \Omega'$ and a narrow-band channel with a Π -shaped characteristic, that transmitted only the frequency $\Omega + \Omega'$. The signals in each channel were handled by either an amplitude or a synchronous detector with a time constant of 3–15 msec. The synchronous detectors were controlled with the aid of signals with the appropriate frequency (Ω or $\Omega + \Omega'$), which varied

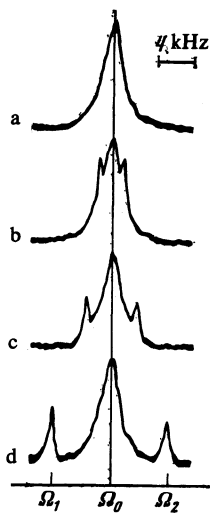


FIG. 3. NMR signals obtained from the protons of water in the RCS at the frequency $\Omega_0/2\pi = 100$ kHz and in the DRCS at the side frequencies Ω_1 and Ω_2 in the case of H_{21} -field frequency (Ω) sweep at fixed H_{31} -field frequency Ω' . $\gamma H_{21} = 710$ Hz for all the curves a)–d); γH_{31} is equal to zero for the curve a) and 200 Hz for the curves b)–d); $\Omega'/2\pi$ is equal to 1.6 kHz for the curve b), 3 kHz for the curve c), and 6.6 kHz for the curve d). The sweep time is equal to 1 sec.

synchronously with the Ω or Ω' sweep. During the Ω' sweep, the frequency Ω was fixed at the value that guaranteed the requisite value of the angle θ' .

B. The NMR signals in the DRCS

The first observation of NMR in the DRCS was performed on protons in water in experiments similar to those in which the NMR in the RCS is directly detected.¹¹ In this case the value of the recording field H_{21} was established in accordance with the condition (2). The adiabatic decrease of the frequency Ω , as the resonance region ($\Omega = \Omega_0$) in the RCS was traversed, was begun immediately after the modulated field H_1 had been adiabatically switched on. In the absence of the second modulation (i.e., for $H_{31} = 0$) what was recorded in this way clearly was the usual NMR dispersion signal u_ρ , greatly broadened by the H_{21} field, in the RCS (Fig. 3a).¹¹ In this case the signal was processed by an amplitude detector. If in such an experiment we switch on in addition a weak field H_{31} with a fixed frequency $\Omega' > \gamma H_{21}$, then in the course of the Ω -frequency sweep the resonance condition (3) in the DRCS will be fulfilled on two occasions, corresponding to detunings Δ' with unlike signs. Figures 3b–3d show the shapes of the signals obtained at different Ω' values. It can be seen that the NMR spectrum exhibits two side lines located symmetrically about the center, i.e., about the frequency Ω_0 , which move away from the center as Ω' increases. The frequencies Ω_1 and Ω_2 of these lines agree well with the values given by the formula

$$\Omega_{1,2} = \Omega_0 \mp [(\Omega')^2 - (\gamma H_{21})^2]^{1/2}, \quad (5)$$

which follows from (3). Consequently, the sideband signals observed by us on the wings of the NMR line in the RCS are a manifestation of resonance in the DRCS.

As follows from (5), the two sideband signals should

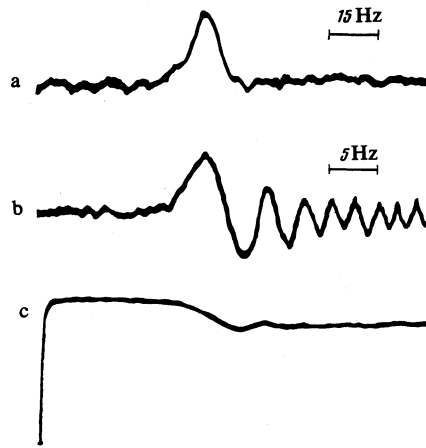


FIG. 4. NMR signals [the curves a) and b)] and a spin-locking signal (the curve c)) respectively obtained at the side frequency $\Omega + \Omega'$ and the frequency Ω from the protons of water in the DRCS [the signals b) and c) were obtained in the same experiment] in the case of Ω' -frequency sweep through the resonance value $\Omega' = \Omega_0'$ and a Ω -frequency detuning relative to Ω_0 of $\Delta' = 0$ in the case a) and $\gamma\Delta' = -100$ Hz for the case b) [$\gamma H_{21} = 3.1$ kHz; $\gamma H_{31} = 1.5$ Hz for the case a) and 0.8 Hz for the case b); the sweep time is equal to 1 sec].

merge into one signal located at the peak of the principal line when $\Omega' = \gamma H_{21}$, and should disappear when $\Omega' < \gamma H_{21}$. The moment of disappearance of the sideband lines turned out to be very sensitive to the value of the frequency Ω' , which allowed us to gauge the H_{21} field with a high degree of accuracy.

To carry out a more detailed study of the NMR effect in the DRCS, we isolated the sideband signal at the frequency $\Omega + \Omega'$ in its pure form. Figure 4a shows an example of the NMR absorption signal v_{pp} in the DRCS from the protons of water, obtained in this way at $\Omega = \Omega_0 = 2\pi \times 100$ kHz (i.e., in the case when $\Delta' = 0$ and $\theta' = 90^\circ$) with the use of the method of Ω' frequency sweep and synchronous detection. It can be seen that the NMR absorption signal v_{pp} in the DRCS is symmetrical, and its width $\Delta\Omega_1'$ at half-maximum is equal to 9 Hz. Although strong suppression of the inhomogeneous broadening is expected at $\theta' = 90^\circ$ (Ref. 12), the observed line width is still quite large, and is due to the H_{21} -field inhomogeneity arising as a result of the inhomogeneity of the H_1 and H_0 fields.

It can be shown that the maximum suppression of the inhomogeneous broadening of the NMR line in the DRCS is attained when the frequency Ω is tuned away from the resonance value Ω_0 by the amount

$$\gamma\Delta' = \Omega_0 - \Omega = \mp [(\gamma H_{21})^2 / \Omega_0] \operatorname{ctg}^2 \theta,$$

where the signs $-$ and $+$ pertain respectively to the cases when the H_{21} field is produced through the modulation of the frequency ω and the amplitude H_1 of the RF field. Figure 4b shows the shape of the NMR signal in the DRCS, as obtained under these conditions in the case of ω modulation for $\gamma\Delta' = -100$ Hz (i.e., for $\theta \approx 92^\circ$). It can be seen that in this case the NMR line in the DRCS is much narrower, and exhibits "wiggles," which are well known in conventional NMR.¹⁷ Because of the inhomogeneity of the H'_{eff} field, the

line broadening in this experiment is altogether about 1 Hz, which is now comparable to the natural width of the line.

C. Spin locking and measurement of the nuclear spin-lattice relaxation time in the DRCS

Figure 4c shows the dispersion signal u_p from the protons of water, as obtained at the frequency $\Omega / 2\pi = 100$ kHz, and processed with the aid of an amplitude detector. This signal was induced in a pickup coil by the magnetization \mathbf{M} oriented along the \mathbf{H}'_{eff} field with the aid of the procedure, described in Sec. 1, for spin locking in the DRCS. Under these conditions $M_{pp\parallel} = M$, and consequently $u_p = M_{p\perp} = M_{pp\parallel} \sin\theta'$, while $v_p = 0$ (see (1) and (4) and Figs. 1 and 2). The NMR signal in the DRCS described in Subsec. 2B and shown in Fig. 4b was recorded at the same time. It can be seen that the "spin-locking signal" shrinks on going through the resonance in the DRCS. This is explained by the irreversible deflection of the magnetization \mathbf{M} from the direction of the \mathbf{H}'_{eff} field at resonance. It can also be seen that during the experiment the spin-lattice relaxation in the DRCS virtually does not decrease the quantity $M_{pp\parallel}$, so that the spin system is virtually isolated from the lattice during this time. As the H_{31} -field intensity was increased, the spin-locking signal shrank further and further right down to the point of its disappearance. This effect is similar to the rotary saturation of NMR in the RCS.^{1,14,15} As the H_{31} field was further increased to values satisfying the condition for fast adiabatic sweep in the DRCS,²⁾ the shrinking of the spin-locking signal became reversible: after passing through the resonance it recovered its original size, and, in the case of synchronous detection, changed its sign. At this point the signal u_{pp} attained its maximum, while the signal v_{pp} vanished, which was to be expected under the conditions of adiabatic passage through the resonance. The width of the dip agreed with the calculated value $\Delta\Omega'_i = 2\gamma h_{31} / \sqrt{3}$ i.e., was three times smaller than the width of the u_{pp} signal at the frequency $\Omega + \Omega'$.

The method of spin locking in the DRCS was also used to measure the spin-lattice relaxation time T_{1pp} in the field H'_{eff} in the DRCS. In these experiments the H_{31} field was found to be equal to zero, and the experiment was of significantly longer duration. Here the spin-locking signal was found to undergo a continuous weakening, which furnished the spin-lattice relaxation curve in the DRCS. Figure 5 shows the result of such an experiment performed on the protons of distilled water at room temperature. It can be seen that the weakening of the spin-locking signal virtually proceeds according to an exponential law with a time constant $T_{1pp} = 3.0 \pm 0.2$ sec, which agrees to within the limits of the experimental error with the measured spin-lattice relaxation times T_1 and T_{1p} in the LCS and RCS respectively. This was to be expected, since the molecular motion in water is characterized by very short correlation times τ_c , so that $\tau_c^{-1} \gg \gamma H'_{\text{eff}}$, γH_{eff} , and γH_0 . At the same time, it is, in practice, very important that only one sweep is necessary for the measurement of T_{1pp} , and that the obtained continuous relaxation curve is not complicated by spurious effects.



FIG. 5. Spin-lattice relaxation curve obtained in the DRCS at the frequency $\Omega / 2\pi = 100$ kHz for the protons of distilled water under conditions of steady spin locking at $\gamma H_{21} = 3.4$ kHz, $\theta' = 90^\circ$. The bottom curve is the zero line.

D. Further suppression of the nuclear dipole-dipole interactions in solids

Figure 6 shows NMR (a) and spin-locking (b) signals in the DRCS from ^{19}F in CaF_2 , obtained in the same way as in the case of Fig. 4 for $\theta = \theta_m$ and $\theta' \approx 92^\circ$. Signals of the type shown in Fig. 6a were also obtained for other values of the angle θ' in the region $0 \leq \theta' \leq 90^\circ$, and the θ' dependence of their width $\Delta\Omega'_i$ is shown in Fig. 7 (let us recall that the condition $\theta = \theta_m$ was consistently maintained here). Figure 7 also shows the corresponding theoretical $2M_{2pp}^{\perp}(\theta')$ curve (where M_{2pp} is the second moment of the NMR absorption line in the DRCS), computed with the aid of the Hamiltonian $\hat{\mathcal{H}}_{dpp}^{(2)}$ without any adjustable parameters whatsoever.¹² It can be seen that the theoretical curve is in good agreement with experiment. In particular, the secular part of the dipole-dipole interactions in the DRCS vanishes in second order perturbation theory as well (i.e., $\hat{\mathcal{H}}_{dpp}^{(2)} = 0$) at the new magic angle $\theta' = 90^\circ$ (Ref. 12). To this corresponds the minimum line width $\Delta\Omega'_i = 10$ Hz (Fig. 6a). This width is 30 times smaller than the previously attained¹¹ minimum NMR line width in the RCS (for its value see the point with $\theta' = 0$ in Fig. 7) and 1.5×10^3 times smaller than the line width in the LCS.¹⁷ Apparently, the residual line width is largely due to the H_1 -field inhomogeneity, which does not allow the condition $\theta = \theta_m$ to be realized simultaneously for all parts of the sample. Let us recall that, as shown in Ref. 12, when $\theta' = \pi/2$ we have suppressed not only the dipole-dipole interactions

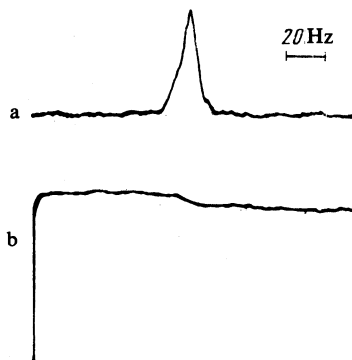


FIG. 6. NMR (a) and spin-locking (b) signals obtained respectively at the side frequency $\Omega + \Omega'$ and the frequency Ω in the DRCS from the ^{19}F nuclei in a CaF_2 single crystal for $\theta = \theta_m$, $\theta' \approx 92^\circ$, $\gamma H_{21} = 3.8$ kHz, $\gamma H_{31} = 0.9$ Hz, and $T = 78$ K in much the same way as the signals shown in Fig. 4 were obtained. The crystal orientation was such that $[111] \parallel H_0$.

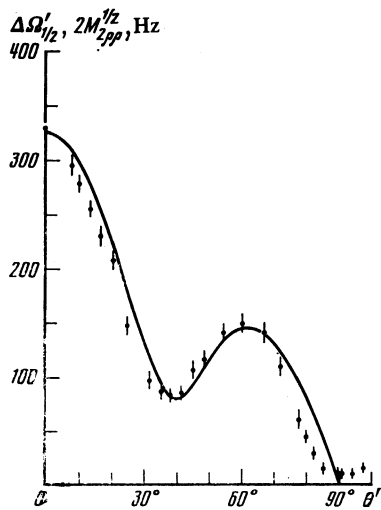


FIG. 7. Experimental NMR-signal width $\Delta\Omega'_1$ in the DRCS (points) and the theoretical value of $2M_{2pp}^{1/2}$, where M_{2pp} is the second moment of the NMR line in the DRCS (curve), for the ^{19}F nuclei in a CaF_2 single crystal as functions of the angle θ' between the directions of the effective fields \mathbf{H}'_{eff} and \mathbf{H}_{eff} in the DRCS in the case of the magic orientation of the field \mathbf{H}_{eff} in the RCS (i.e., for $\theta = \theta_m$). The crystal orientation was such that $[111] \parallel \mathbf{H}_0$; $\gamma H_{21} = 3.8$ kHz.

of the spins I , but also the chemical shifts and the dipole interactions with any other types of spins (nuclear and electronic) present in the sample. The indirect scalar spin-spin interactions with the other types of nuclei should also be suppressed, just as such interactions are suppressed by a strong strictly resonance H_1 field.¹⁷

As predicted by theory,¹² the θ' dependence of $\Delta\Omega'_1$ also has a local minimum at $\theta' = \theta'_0 = \arccos(\frac{3}{5})^{1/2} \approx 39^\circ 12'$. Here, however, the line width is significantly greater than the line width for $\theta' = \pi/2$, and is about 70 Hz. But then the chemical shift does not vanish under these conditions (as happens at $\theta' = \pi/2$), and is only $(\cos \theta_m \cdot \cos \theta'_0)^{-1} = \sqrt{5}$ times smaller than the shift in the LCS.¹² Therefore, it is most advantageous to use precisely this value of θ' in chemical-shift resolution experiments performed on solids.

It follows from Fig. 7 that, in the region $0 \leq \theta' \leq 88^\circ$, the ratio $\Delta\Omega'_1/2M_{2pp}^{1/2} \leq 1$. This practically coincides with the analogous ratio in the RCS for the same orientation of the CaF_2 crystal,¹¹ but differs significantly from the ratio in the LCS, where $\Delta\omega_1/2M_{2pp}^{1/2} = 1.26$ (Ref. 17). This indicates that, for $\theta = \theta_m$, the NMR line has different shapes in the LCS and DRCS.

Let us note that an experimental curve of the type shown in Fig. 7 exhibited a steep dip at $\theta' = \arccos(1/\sqrt{3}) = 54^\circ 44'$ in the cases when the angle θ was slightly different from θ_m . This dip is due to the suppression in the DRCS of the first-order secular dipole-dipole interactions, which acquire the factor $(3 \cos^2 \theta - 1)(3 \cos^2 \theta' - 1)$ on being transformed from the RCS into the DRCS. It can be used to check the preciseness of the θ and θ' adjustments.

3. CONCLUSION

Thus, the observation of the NMR in the DRCS ensures the narrowing of the resonance line in solids down to values

of the order of 10 Hz, which is comparable to what is attained with the most modern multipulsed methods.⁴ In our case the NMR frequency spectrum is obtained at one in the final form, requiring no Fourier transformation, and the transmitter power (about 30 W) is one-to-two orders of magnitude lower than the power required in the multipulsed experiments.^{8,9} As to the sensitivity, it is apparently somewhat lower than that attained in the traditional methods, but, as can be seen from Fig. 4–6, it is quite adequate for the measurements. It can, if necessary, be easily raised through the raising of the \mathbf{H}_0 -field intensity and (or) the buildup of the signal.

At the same time it should be noted that the spectroscopic applications of our method are limited under maximal-narrowing conditions (i.e., when $\theta' = \pi/2$). Information about the chemical shifts can be obtained only at the cost of broadening of the line up to ≈ 70 Hz (i.e., only in experiments with $\theta' = \arccos(\frac{3}{5})^{1/2}$).

In this connection we would like to bring out another important aspect of the present investigation, namely, the steady spin locking the DRCS, which allows us to measure in one sweep a new relaxation parameter: the nuclear spin-lattice relaxation time T_{1pp} in the \mathbf{H}'_{eff} field in the DRCS. In the $\theta, \theta' \neq \theta_m$ case, when the nuclear dipole-dipole interactions are not significantly suppressed, the time T_{1pp} should contain essentially the same information about the internal atomic-molecular motions as T_{1p} (and, for liquids, T_1). Considering the fact that the point-by-point measurement of the time T_{1p} is extremely laborious,^{1,2} and that the use for this purpose of pulsed spin locking in the RCS is complicated by spurious multispin transitions,^{5,6} the method described in the present paper is more convenient.

Even more important is the fact that, for $\theta = \theta_m$, the condition $H_{Lp} \ll H'_{\text{eff}} \ll H_{\text{eff}}$ is easily realized in solids, and in this case the time T_{1pp} will be especially sensitive to the extremely slow internal motions with $\tau_c^{-1} \sim \gamma H'_{\text{eff}} \sim 10^2 - 10^4$ Hz. Let us note that such motions are difficult to study with the aid of the standard T_{1p} measurements in the RCS, measurements which furnish the greatest amount of information when $\tau_c^{-1} \sim \gamma H_{\text{eff}} \approx 10^4 - 10^5$ Hz (Refs. 1–4).

Thus, it may be hoped that the recording of NMR and the study of nuclear relaxation in the DRCS will become a useful tool of investigation of the structure and internal atomic-molecular motions in solids and liquids.

The author thanks V. A. Ațsarkin for a discussion of the results and for valuable comments and M. I. Kalinin for his help in the investigation.

¹¹The oblique DRCS will hereafter simply be called the DRCS.

¹²In the DRCS this condition has the form $T_{2pp}^{-1} \ll (\gamma H_{31})^{-1} d\Omega'/dt \ll \gamma H_{31}$, where T_{2pp} is the transverse relaxation time in the DRCS, and differs from the corresponding condition in the LCS¹⁷ only in that, instead of the parameters H_1 , ω , and T_2 , we now have figuring in the condition the parameters H_{31} , Ω' , and T_{2pp} .

¹³M. Goldman, Spin Temperature and Nuclear Magnetic Resonance in Solids, Clarendon Press, Oxford, 1970 (Russ. Transl., Mir, Moscow, 1972).

- ²T. C. Farrar and E. D. Becker, *Pulse and Fourier Transform NMR*, Academic Press, New York, 1971 (Russ. Transl., Mir, Moscow, 1973).
- ³J. S. Waugh, *New Methods of NMR in Solids*, Acad. Pr., New York (Russ. Transl., Mir, Moscow, 1978).
- ⁴U. Haerberlen and M. Mering, *High Resolution NMR in Solids*, Academic, 1976 (Russ. Transl., Mir, Moscow, 1980).
- ⁵L. N. Erofeev, B. A. Shumm, and G. B. Manelis, *Zh. Eksp. Teor. Fiz.* **75**, 1837 (1978) [Sov. Phys. JETP **48**, 925 (1978)].
- ⁶Yu. N. Ivanov, B. N. Provotorov, and É. B. Fel'dman, *Zh. Eksp. Teor. Fiz.* **75**, 1847 (1978) [Sov. Phys. JETP **48**, 930 (1978)].
- ⁷B. N. Provotorov and É. B. Fel'dman, *Zh. Eksp. Teor. Fiz.* **79**, 2206 (1980) [Sov. Phys. JETP **52**, 1116 (1980)].
- ⁸J. D. Ellett *et al.*, *Adv. Magn. Reson.* **5**, 117 (1971).
- ⁹L. N. Erofeev, O. D. Vetrov, B. A. Shumm, M. Sh. Isaev, and G. B. Manelis, *Prib. Tekh. Eksp. No. 2*, 145 (1977).
- ¹⁰D. P. Burum, M. Linder, and R. R. Ernst, *J. Magn. Reson.* **44**, 173 (1981).
- ¹¹A. E. Mefèd and V. A. Atsarkin, *Zh. Eksp. Teor. Fiz.* **74**, 720 (1978) [Sov. Phys. JETP **47**, 378 (1978)].
- ¹²V. A. Atsarkin, A. E. Mefèd, and M. I. Rodak, *Fiz. Tverd. Tela* **21**, 2672 (1979) [Sov. Phys. Solid State **21**, 1537 (1979)].
- ¹³A. E. Mefèd and M. I. Kalinin, *Problemy magnit. reson. Tezisy dokl. 7 Vsesoyuznoi shkoly po magnit. reson. (Problems of Magnetic Resonance: Abstracts of Papers Presented at the Seventh All-Union School on Magnetic Resonance)*, Slavyanogorsk, 1981, p. 108.
- ¹⁴A. G. Redfield, *Phys. Rev.* **98**, 1787 (1955).
- ¹⁵J. R. Franz and C. P. Slichter, *Phys. Rev.* **148**, 287 (1966).
- ¹⁶M. Lee and W. I. Goldberg, *Phys. Rev. A* **140**, 1261 (1965).
- ¹⁷A. Abragam, *The Principles of Nuclear Magnetism*, Clarendon Press, Oxford, 1961 (Russ. Transl., IIL, Moscow, 1963).
- ¹⁸V. G. Pokazan'ev and L. I. Yakub, *Zh. Eksp. Teor. Fiz.* **73**, 221 (1977) [Sov. Phys. JETP **46**, 114 (1977)].

Translated by A. K. Agyei